

Uncertainty-Aware Surrogate for Fatigue Assessment of Moorings in Offshore Wind Turbines

Rohit Kumar¹, Arvind Keprate², and Subhamoy Sen³

^{1,3} *i4S Laboratory, Indian Institute of Technology Mandi, Mandi, HP, India*
rohit373k@gmail.com
subhamoy@iitmandi.ac.in

² *Green Energy Lab, Department of Mechanical, Electrical and Chemical Engineering, Oslo Metropolitan University, Oslo, Norway*
arvindke@oslomet.no

ABSTRACT

Floating Offshore Wind Turbines (FOWTs) deployed in deep waters extract wind energy via floating platforms that are station kept by mooring lines subjected to complex, highly dynamic loading conditions. The cyclic nature of these dynamic loads induces fatigue damage in the mooring lines, which can culminate in catastrophic failures with substantial operational, economic, and safety implications. The remote offshore location of FOWTs renders conventional, sensor-intensive structural health monitoring in deep water both costly and logistically challenging. Indirect sensing approaches offer a promising alternative; however, existing methods typically neglect inherent aleatoric material uncertainties arising from manufacturing variability, installation effects, and long-term corrosion, thereby limiting their reliability for informed decision making.

To overcome this limitation, the present study introduces an uncertainty-aware surrogate-based indirect sensing framework that quantifies mooring line fatigue damage in a fully probabilistic manner by constructing confidence regions of damage conditional on the prevailing environmental loading. This probabilistic characterization supports more reliable, risk informed inspection, maintenance planning, and life-extension strategies. The surrogate model is trained over a wave scatter table representative of the Gulf of Khambhat region, encompassing a wide range of sea states. Training and validation datasets are generated using high fidelity numerical simulations generated with OpenFAST, based on the NREL 5 MW OC4 semisubmersible wind turbine reference model.

Rohit Kumar et al. This is an open-access article distributed under the terms of the Creative Commons Attribution 3.0 United States License, which permits unrestricted use, distribution, and reproduction in any medium, provided the original author and source are credited.

1. INTRODUCTION

Floating Offshore Wind Turbines (FOWTs) enable wind energy extraction in deepwater environments, thereby providing access to stronger and more consistent wind resources (Grasu & Liu, 2023). Station keeping for FOWTs is achieved through mooring systems that anchor the floating platform to the seabed. These mooring lines are subjected to coupled stochastic environmental loads from wind, waves, and currents, resulting in significant platform motions and dynamic tension variations (Fontaine et al., 2014).

The cyclic tension experienced by mooring lines induces progressive fatigue damage, which can lead to premature failure over the operational lifetime of FOWTs. Such failures may compromise station keeping, resulting in excessive platform drift, operational downtime, or even catastrophic system collapse, thereby posing significant safety, environmental, and economic risks (Grasu & Liu, 2023). However, monitoring the condition of mooring lines in offshore environments remains challenging due to their deep water location and exposure to harsh marine conditions, which hinder direct inspection and make sensor deployment costly. Various sensing technologies, including load cells, Fiber Bragg Grating sensors and acoustic emission sensors, have been proposed for mooring system monitoring (Yang, Chen, Liu, & Liu, 2010; Minnebo, Aalberts, & Duggal, 2014). Nevertheless, the installation, calibration, and long term maintenance of such sensing infrastructure require specialized subsea operations, resulting in significant logistical complexity and operational costs.

To overcome the limitations of direct sensing, model based and indirect sensing approaches have gained increasing attention. Physics based numerical models can estimate mooring loads and fatigue damage under varying environmental conditions, particularly through high fidelity simulations that capture the coupled aero-hydro-servo-elastic behavior of float-

ing wind turbines (Thakur et al., 2025; Kumar, Thakur, O A, Keprate, & Sen, 2024). However, their application becomes computationally demanding when large numbers of simulations are required, such as in fatigue assessment across environmental wave scatter table.

In this context, indirect sensing has emerged as a promising alternative. These approaches combine limited measurements such as platform motion, wind speed, and acceleration with data driven surrogates or physics-informed models to estimate unmeasured quantities like mooring tension (Thakur et al., 2025; Kumar et al., 2024). Recent studies have demonstrated the effectiveness of machine learning techniques, including LSTM-based models and lidar assisted frameworks, in accurately predicting mooring loads (Gräfe, Pettas, Dimitrov, & Cheng, 2024). Additionally, indirect sensing methods have been successfully extended to complex FOWT configurations, enabling the estimation of both mooring loads and structural responses using a reduced set of sensors (del Pozo Gonzalez, Kallinger, Yalcin, Rapha, & Domínguez-García, 2025).

In parallel, surrogate modeling techniques have been developed to reduce the computational cost of high fidelity simulations. These models approximate the relationship between environmental inputs and structural responses using a limited set of simulations, making them well suited for indirect sensing applications. Methods such as polynomial response surfaces, neural networks, and Gaussian process regression (Kriging) enable rapid prediction of loads and fatigue damage without repeated simulations (Kumar, Prasad, Keprate, & Sen, 2025; Tandon & Sen, 2025; Arya, Kumar, Keprate, & Sen, 2025; Kumar, Thakur, Sen, & Keprate, 2026).

However, most existing surrogate modeling approaches assume deterministic system parameters and do not explicitly account for uncertainties in mooring systems. In practice, variability due to manufacturing tolerances, installation conditions, and degradation processes such as corrosion can significantly influence fatigue response (Xu, Guedes Soares, & Teixeira, 2018). Neglecting these uncertainties may lead to inaccurate fatigue predictions and non-conservative assessments. Incorporating uncertainty quantification into surrogate modeling is therefore essential for developing reliable damage assessment frameworks. Probabilistic modeling approaches can provide confidence intervals or distributions for predicted responses, enabling risk informed decision making in inspection and maintenance planning. However, conventional surrogate models often focus solely on mean response prediction and are not designed to explicitly represent stochastic variability present in simulation outputs or material properties.

To address this limitation, the present study extends the stochastic Kriging framework previously developed for uncertainty-aware peak mooring tension prediction (Kumar, Prasad, et al., 2025) toward fatigue damage assessment of FOWT moor-

ing systems. The proposed approach functions as an indirect sensing framework by establishing a surrogate relationship between environmental sea states and the corresponding mooring fatigue damage response while explicitly quantifying the associated uncertainty. Unlike conventional deterministic surrogates, stochastic Kriging captures both the mean fatigue response and the stochastic variability arising from environmental and system uncertainties (Ankenman, Nelson, & Staum, 2008). Consequently, the developed framework enables rapid probabilistic evaluation of mooring fatigue damage across the environmental wave scatter table together with associated confidence bounds, thereby supporting uncertainty-informed reliability assessment and maintenance planning.

The remainder of this paper is organized as follows. Section 2 outlines the stochastic Kriging surrogate methodology and describes dataset generation and model training. Section 3 presents the results and discussion, followed by conclusions in Section 4.

2. METHODOLOGY

Stochastic Kriging is a spatial interpolation technique for modeling stochastic systems with inherent output variability. It explicitly accounts for intrinsic uncertainty arising from both mooring material properties (modeled here as axial stiffness with a coefficient of variation ($\text{cov} = 0.05$) (Kumar, Prasad, et al., 2025)) and environmental randomness, represented by multiple wave realizations corresponding to a given sea state in the wave scatter table.

The dataset used for training and validation of the surrogate model is generated through high fidelity simulations of a representative FOWT, as described later in this section. Specifically, the NREL OC4 semisubmersible platform (Robertson et al., 2014) is modeled in OPENFAST (Jonkman et al., 2022) to capture the coupled aero-hydro-servo-elastic response under varying wave conditions. The stochastic Kriging surrogate is then constructed to map key environmental inputs, such as significant wave height and peak period, to the corresponding fatigue damage.

Let $\mathbf{x} \in \mathbb{R}^p$ denote the vector of input variables describing the environmental conditions. In this study, \mathbf{x} represents the environmental state parameters obtained from the wave scatter table. A set of n design points in the input space is selected and denoted as

$$\mathcal{X}^d = \{\mathbf{x}_1^d, \mathbf{x}_2^d, \dots, \mathbf{x}_n^d\}. \quad (1)$$

At each design point \mathbf{x}_i^d , multiple high fidelity simulations are performed to evaluate the corresponding fatigue damage in the mooring line. Let the output from the j -th simulation at the i -th design point be

$$y_{ij}^d, \quad j = 1, 2, \dots, r_i, \quad (2)$$

where r_i is the number of replications at that design point. Since the input conditions are fixed but the outputs are influenced by stochastic wave realizations and mooring material and handling variability, the results at each design point are treated as random variables. The sample mean fatigue damage at \mathbf{x}_i^d is computed as

$$\bar{y}_i^d = \frac{1}{r_i} \sum_{j=1}^{r_i} y(\mathbf{x}_{i,j}^d) \quad (3)$$

and the corresponding sample variance is

$$\sigma_i^{d2} = \frac{1}{r_i - 1} \sum_{j=1}^{r_i} (y_{ij}^d - \bar{y}_i^d)^2 \quad (4)$$

The vector of observed fatigue damage outputs for all design points is then given as

$$\bar{\mathbf{y}}^d = [\bar{y}_1^d, \bar{y}_2^d, \dots, \bar{y}_n^d]^T, \quad (5)$$

2.1. Stochastic Kriging Model

The underlying response at any input location $\mathbf{x} \in \mathbb{R}^p$ is modeled as

$$y(\mathbf{x}) = \mathbf{B}(\mathbf{x})^T \boldsymbol{\beta} + \mathcal{M}(\mathbf{x}) + \varepsilon(\mathbf{x}), \quad (6)$$

where $\mathbf{B}(\mathbf{x}) \in \mathbb{R}^q$ is a vector of predefined basis functions, $\boldsymbol{\beta} \in \mathbb{R}^q$ is the vector of regression coefficients, $\mathcal{M}(\mathbf{x})$ is a zero-mean Gaussian process representing spatial correlation (extrinsic uncertainty), and $\varepsilon(\mathbf{x})$ denotes intrinsic uncertainty arising from stochastic simulation variability.

The intrinsic uncertainty is characterized by analyzing the variability in simulation outputs across multiple replications at each design point \mathbf{x}_i^d . Since the stochastic component $\varepsilon(\mathbf{x})$ varies with the input location, the intrinsic variance is not uniform across the design space. The variance associated with the i -th design point is denoted as $\sigma_{\varepsilon,i}^2 = \text{Var}[\varepsilon(\mathbf{x}_{i,j}^d)] \forall j > 0$.

The Gaussian process $\mathcal{M}(\mathbf{x})$ is characterized by its covariance function

$$\text{Cov}[\mathcal{M}(\mathbf{x}_i^d), \mathcal{M}(\mathbf{x}_j^d)] = \delta^2 R(\mathbf{x}_i^d, \mathbf{x}_j^d), \quad (7)$$

where δ^2 is the process variance and $R(\cdot, \cdot)$ is the correlation function. Based on semivariogram analysis (Fig. 3), a Gaussian correlation model is adopted to represent the smooth dependence of fatigue damage on environmental inputs:

$$R(\mathbf{x}_i^d, \mathbf{x}_j^d) = \exp\left(-\sum_{h=1}^p \theta_h (x_{i,h}^d - x_{j,h}^d)^2\right), \quad (8)$$

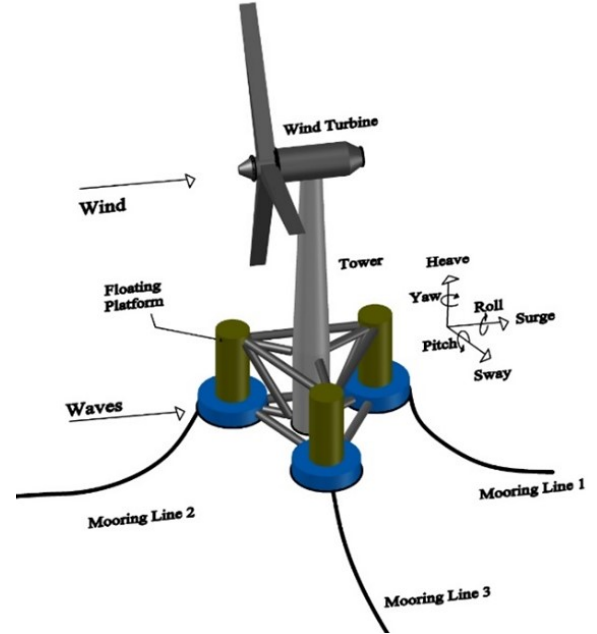


Figure 1. OC4 semisubmersible platform and mooring lines

where $x_{i,h}^d$ denotes the h -th input feature of the input vector at the i -th design point, $h = 1, \dots, p$, and θ_h are the corresponding correlation length scale parameters.

Let $\mathbf{R} \in \mathbb{R}^{n \times n}$ denote the correlation matrix with entries $R_{ij} = R(\mathbf{x}_i^d, \mathbf{x}_j^d)$, and let $\boldsymbol{\Sigma}_\varepsilon = \text{diag}(\sigma_{\varepsilon,1}^2, \dots, \sigma_{\varepsilon,n}^2)$ represent the intrinsic noise covariance matrix. The total covariance matrix of the observed responses is then given by

$$\boldsymbol{\Sigma} = \delta^2 \mathbf{R} + \boldsymbol{\Sigma}_\varepsilon. \quad (9)$$

The model parameters $\boldsymbol{\beta}$, δ^2 , and $\boldsymbol{\theta} = \{\theta_1, \dots, \theta_p\}$ are estimated by the log-likelihood function, given by

$$\begin{aligned} \mathcal{L}(\delta^2, \boldsymbol{\theta}) = & -\frac{1}{2} \left[n \log(2\pi) + \log |\boldsymbol{\Sigma}| \right. \\ & \left. + (\bar{\mathbf{y}}^d - \mathbf{B}(\mathbf{x}^d) \boldsymbol{\beta})^T \boldsymbol{\Sigma}^{-1} (\bar{\mathbf{y}}^d - \mathbf{B}(\mathbf{x}^d) \boldsymbol{\beta}) \right] \end{aligned} \quad (10)$$

A detailed mathematical formulation of the estimation procedure is provided in (Kumar, Prasad, et al., 2025).

For a new prediction point \mathbf{x}^p , define the correlation vector $\mathbf{r}(\mathbf{x}^p) \in \mathbb{R}^n$ with entries

$$r_i(\mathbf{x}^p) = R(\mathbf{x}^p, \mathbf{x}_i^d), \quad i = 1, \dots, n. \quad (11)$$

The stochastic Kriging predictor for the mean response is then given by

$$\hat{y}(\mathbf{x}^p) = \mathbf{B}(\mathbf{x}^p)^T \hat{\boldsymbol{\beta}} + \delta^2 \mathbf{r}(\mathbf{x}^p)^T \boldsymbol{\Sigma}^{-1} (\bar{\mathbf{y}}^d - \mathbf{B}(\mathbf{x}^d) \hat{\boldsymbol{\beta}}), \quad (12)$$

where $\mathbf{B}(\mathbf{x}^d) \in \mathbb{R}^{n \times q}$ is the matrix of basis functions evaluated at all design points.

Table 1. Sea state scatter table for the Gulf of Khambhat showing the occurrence of sea states as a function of significant wave height (H_s) and peak wave period (T_p)

H_s [m]	T_p [s]																										
	0.5	1.5	2.5	3.5	4.5	5.5	6.5	7.5	8.5	9.5	10.5	11.5	12.5	13.5	14.5	15.5	16.5	17.5	18.5	19.5	20.5	21.5	22.5	23.5	24.5	25.5	
2.75	0	0	0	0	0	0	0	0	0	9	60	197	112	36	3	0	0	0	0	0	0	0	0	0	0	0	0
2.25	0	0	0	0	0	0	2	1	10	237	1738	1464	242	13	0	1	6	5	4	0	0	0	0	0	0	0	0
1.75	0	0	0	0	0	23	17	25	460	1927	2628	809	66	26	25	51	31	17	5	3	0	0	0	0	0	0	0
1.25	0	0	0	3	139	65	131	301	1178	1459	372	193	426	567	481	376	127	67	43	7	8	1	1	1	0	0	1
0.75	0	0	88	2301	387	258	453	509	332	195	899	2221	3120	2689	1904	1208	390	211	127	33	11	0	0	0	0	0	0
0.25	0	15	656	754	155	79	96	78	130	733	1491	1817	1578	1158	714	528	189	63	29	11	6	3	0	0	0	0	2

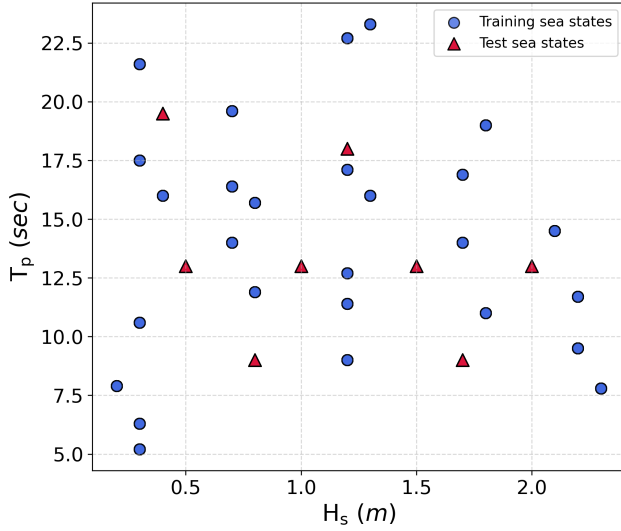


Figure 2. Training and testing design points

2.2. Dataset Generation

The present study considers a 5 MW NREL-OC4 DeepCwind semi-submersible floating offshore wind turbine installed at a water depth of 200 m. The turbine is supported by an OC4 semi-submersible platform (Robertson et al., 2014) (Fig. 1) and moored using three catenary lines of 76.6 mm diameter, arranged at 120° spacing (Fig. 2). Detailed specifications of the turbine and platform are provided in (Kumar, Sen, & Keprate, 2025). High-fidelity numerical simulations are conducted using OpenFAST, an open-source tool for fully coupled aero-hydro-servo-elastic analysis of offshore wind systems (Jonkman et al., 2022).

Irregular waves are represented using the JONSWAP spectrum (Kumar, Sen, & Keprate, 2025), and environmental conditions are selected to reflect the Gulf of Khambhat, Gujarat, as summarized in Table 1 (National Institute of Wind Energy (NIWE), 2017). Each sea state is defined by significant wave height (H_s) and peak wave period (T_p), which serve as the primary input variables for the surrogate model (Fig. 2). A total of 35 sea states are considered, with 27 used for training and 8 reserved for testing and validation.

Simulations are performed at a constant wind speed of 8 m/s and without current to isolate wave-induced mooring loads,

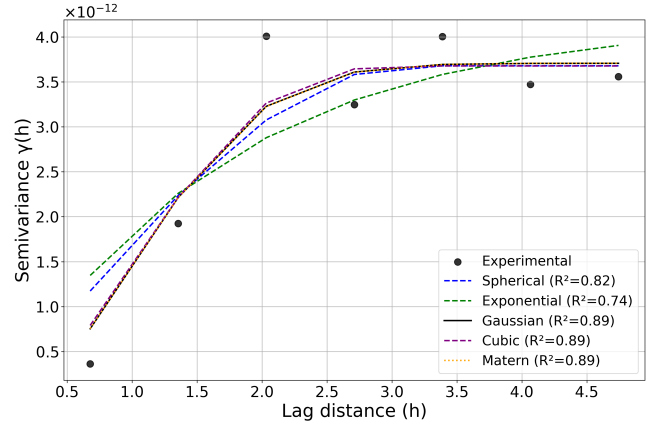


Figure 3. Semivariogram model for different model assumptions for spatial correlation

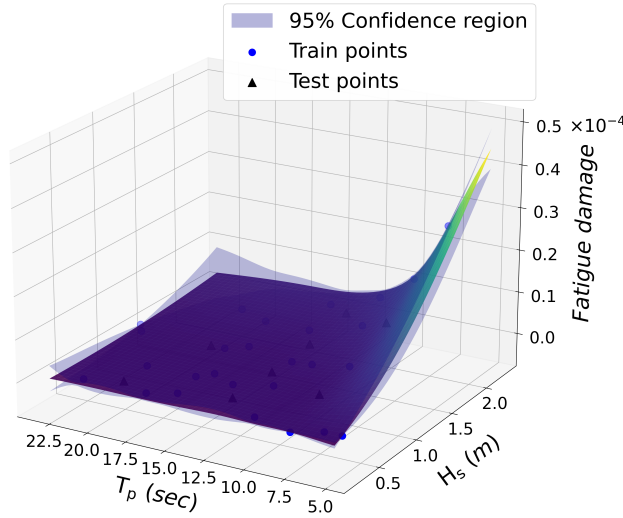
which are the primary contributors to fatigue. The wind and wave directions are kept aligned, and only a single environmental direction is considered. Accordingly, the surrogate model is formulated as a function of H_s and T_p , reducing the input dimensionality while retaining the dominant sources of fatigue variability. To account for stochasticity, 100 independent simulations are conducted for each sea state, resulting in 3,500 simulations over 35 design points. After discarding the initial transient, a continuous 3-hour segment of steady-state mooring tension history is used to compute fatigue damage via the rainflow counting method with a bin size of 1 kN. Previous studies have indicated that bin sizes of up to 3 kN provide sufficient accuracy for fatigue cycle characterization (Kumar, Sen, & Keprate, 2025). The mooring lines are modeled as R4-grade studless chains, and cycles with tension ranges below the material endurance limit are excluded from the analysis to ensure that only fatigue relevant cycles contribute to damage accumulation.

3. RESULTS AND DISCUSSION

A key component of stochastic Kriging is the modeling of spatial correlation through the variogram or covariance structure. Several candidate variogram models were evaluated, including spherical, exponential, and Gaussian functions. Figure 3 shows the fitted semivariogram models. Although the candidate models exhibited comparable performance, the Gaussian variogram was selected due to its slightly better fit and

Table 2. Designed Stochastic Kriging Metamodel parameters

Design parameters	
Input	$[H_s, T_p]$
Output	Fatigue Damage (μ, σ)
Trend	
Type	Quadratic
Beta	$[4.702 \times 10^{-6}, 8.871 \times 10^{-6}, -1.162 \times 10^{-6}, 2.337 \times 10^{-6}, 5.667 \times 10^{-8}, -7.830 \times 10^{-7}]$
Hyperparameters	
Correrationion	Gaussian
δ^2	1.356×10^{-9}
θ	$[0.124, 0.033]$
Optimization Method	L-BFGS-B



(a) Interpolated surface with confidence interval using stochastic Kriging

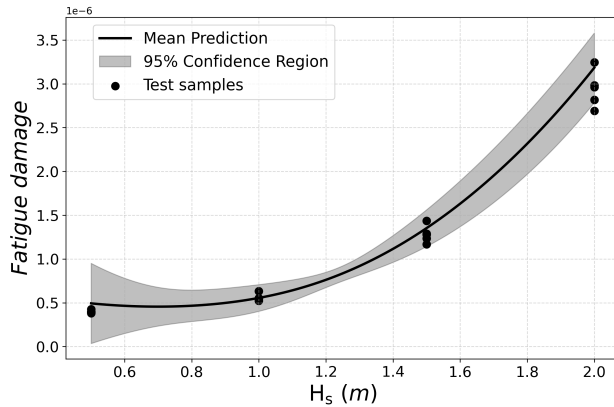

 (b) Test data falling within confidence region of interpolated region for $T_p = 13$ s

Figure 4. Interpolated surface for fatigue damage at mooring line 1 using Stochastic Kriging

Table 3. Performance Metrics of Stochastic Kriging model for train, test, and all simulation data

Criteria	Train data	Test data	All data
R^2	0.999	0.989	0.999
RMSE	3×10^{-7}	7×10^{-6}	8×10^{-7}
NRMSE (%)	9.282	13.711	10.640
CR	0.926	0.872	0.908

smoother interpolation characteristics, with an R^2 value of 0.89. This result indicates that the Gaussian model effectively captures the spatial dependence of fatigue damage across the (H_s, T_p) input space; therefore was adopted in the final stochastic Kriging surrogate.

The estimated stochastic Kriging model parameters are summarized in Table 2. The regression coefficients β represent the deterministic trend component of the surrogate model, while the correlation parameters θ determine the spatial smoothness of the Gaussian process. The process variance δ^2 characterizes the magnitude of epistemic uncertainty in the response surface. The relatively small process variance indicates that the surrogate model provides a stable approximation of the fatigue response surface within the considered input domain.

Using the trained stochastic Kriging model, a continuous fatigue damage surface was constructed over the (H_s, T_p) domain for the mooring line. Figure 4a illustrates the predicted fatigue damage surface along with the associated uncertainty bounds obtained from the surrogate prediction variance for mooring line 1. Similar fatigue damage surfaces can likewise be developed for the remaining mooring lines, although they are not presented here.

The results illustrate the strong dependence of fatigue damage on both wave height and wave period. In general, fatigue damage increases with increasing H_s due to the larger dynamic loads induced by higher waves. The influence of T_p is more complex and is related to the interaction between the wave excitation frequency and the dynamic characteristics of the floating structure.

The uncertainty bounds shown in the figure represent the combined effects of epistemic uncertainty associated with limited training data and aleatoric uncertainty arising from stochastic simulation variability. Regions with sparse training data exhibit larger uncertainty, while areas near the design points show tighter confidence bounds.

To provide further insight into the surrogate model predictions, a cross-sectional analysis was performed by fixing the peak wave period at $T_p = 13$ s and varying the significant wave height H_s . Figure 4b shows the predicted fatigue damage curve along with the uncertainty bounds and the corresponding test samples. The results show that most of the test data points fall within the predicted probabilistic region, confirming the predictive capability of the stochastic Kriging surrogate. The uncertainty band widens slightly at larger values

of H_s , reflecting increased variability in fatigue damage under more energetic sea states.

The predictive performance of the stochastic Kriging model is evaluated on an independent test dataset using standard error metrics, including the root mean square error (RMSE), coefficient of determination (R^2), and normalized RMSE (NRMSE), as summarized in Table 3. The high coefficient of determination ($R^2 = 0.989$) indicates that the surrogate model captures the majority of the variability in the fatigue damage data. The low RMSE values further demonstrate the accuracy of the surrogate predictions relative to the magnitude of the fatigue damage values.

To further evaluate the reliability of the uncertainty predictions, the containing ratio (CR) was computed. The CR represents the proportion of data points enclosed within the predicted 95% confidence intervals of the surrogate model, for which the ideal expected coverage is 95%. The results indicate that the majority of the test samples fall within the predicted uncertainty bounds, demonstrating that the stochastic Kriging model provides reasonably well-calibrated probabilistic predictions. This demonstrates that the surrogate model successfully captures both the mean fatigue response and the associated uncertainty across the input space.

The proposed indirect fatigue damage sensing framework based on stochastic Kriging surrogate performs reliably within the range of environmental conditions represented in the training data and can be further enhanced by incorporating additional input variables and real-time updates. Its performance depends on the quality of the underlying simulations and can be improved with better data and a wider range of operating conditions.

4. CONCLUSIONS

The stochastic Kriging model demonstrates strong predictive capability in capturing both fatigue damage and its associated uncertainty across the environmental space. Its ability to provide rapid and probabilistically consistent estimates enables its use as an indirect sensing framework for mooring fatigue assessment, delivering fatigue predictions directly from recorded sea states without the need for physical instrumentation or repeated high-fidelity simulations. This facilitates continuous uncertainty-informed monitoring of mooring system integrity and supports reliable risk-informed decision making. Future work will focus on reliability analysis for probabilistic failure assessment and integration with real-time operational data for adaptive monitoring. Although the present framework has been demonstrated under simplified conditions with a constant wind speed, no current, and a single aligned wind-wave direction, the methodology can be extended to incorporate more realistic environmental and operational conditions.

REFERENCES

- Ankenman, B., Nelson, B. L., & Staum, J. (2008). Stochastic kriging for simulation metamodeling. In *2008 winter simulation conference* (p. 362-370). doi: <https://doi.org/10.1109/WSC.2008.4736089>
- Arya, A., Kumar, R., Keprate, A., & Sen, S. (2025, Nov.). Real-time monitoring of clump weight integrity loss in floating wind turbines via deep learning. *Journal of Dynamics, Monitoring and Diagnostics*. doi: [10.37965/jdmd.2025.792](https://doi.org/10.37965/jdmd.2025.792)
- del Pozo Gonzalez, H., Kallinger, M. D., Yalcin, T., Rapha, J. I., & Domínguez-García, J. L. (2025). Design of virtual sensors for a pyramidal weathervaning floating wind turbine. *Journal of Marine Science and Engineering*, *13*(8). doi: [10.3390/jmse13081411](https://doi.org/10.3390/jmse13081411)
- Fontaine, E., Kilner, A., Carra, C., Washington, D., Ma, K., Phadke, A., ... Kusinski, G. (2014). Industry survey of past failures, pre-emptive replacements and reported degradations for mooring systems of floating production units. In *Offshore technology conference* (p. D041S047R002). doi: <https://doi.org/10.4043/25273-MS>
- Gräfe, M., Pettas, V., Dimitrov, N., & Cheng, P. W. (2024). Machine-learning-based virtual load sensors for mooring lines using simulated motion and lidar measurements. *Wind Energy Science*, *9*(11), 2175–2193. doi: <https://doi.org/10.5194/wes-9-2175-2024>
- Grasu, G., & Liu, P. (2023). Risk assessment of floating offshore wind turbine. *Energy Reports*, *9*, 1–18. doi: <https://doi.org/10.1016/j.egy.2022.11.147>
- Jonkman, B., Mudafort, R. M., Platt, A., Branlard, E., Sprague, M., jjonkman, ... rcorniglian (2022, March). *Openfast/openfast: Openfast v3.1.0*. Zenodo.
- Kumar, R., Prasad, K. J., Keprate, A., & Sen, S. (2025). Addressing material uncertainty in reliability analysis of floating offshore mooring through probabilistic meta-model developed with stochastic kriging technique. *Ocean Engineering*, *335*, 121697. doi: <https://doi.org/10.1016/j.oceaneng.2025.121697>
- Kumar, R., Sen, S., & Keprate, A. (2025). Real-time fatigue assessment of floating offshore wind turbine mooring employing sequence-to-sequence-based deep learning on indirect fatigue response. *Ocean Engineering*, *315*, 119741. doi: <https://doi.org/10.1016/j.oceaneng.2024.119741>
- Kumar, R., Thakur, A., O A, S., Keprate, A., & Sen, S. (2024). Characterizing damage in wind turbine mooring using a data-driven predictor model within a particle filtering estimation framework. In *Proceedings of the phm society european conference* (Vol. 8, p. 8). doi: <https://doi.org/10.36001/phme.2024.v8i1.4051>
- Kumar, R., Thakur, A., Sen, S., & Keprate, A. (2026). Temporal feature extraction based real time damage detec-

- tion of floating offshore wind turbine mooring lines. In M. Singh et al. (Eds.), *Proceedings of the unified conference of damas, income viii and tepen conferences* (pp. 59–68). Cham: Springer Nature Switzerland. doi: <https://doi.org/10.1007/978-3-031-95963-9>
- Minnebo, J., Aalberts, P., & Duggal, A. (2014). Mooring system monitoring using dgps. In *International conference on offshore mechanics and arctic engineering* (Vol. 45387, p. V01BT01A035). doi: <https://doi.org/10.1115/OMAE2014-24401>
- National Institute of Wind Energy (NIWE). (2017, September). *Fowpi – metocean study* (Tech. Rep. No. A073635-014-001). India: National Institute of Wind Energy. (Project No. A073635, First Issue)
- Robertson, A., Jonkman, J., Masciola, M., Song, H., Goupee, A., Coulling, A., & Luan, C. (2014). *Definition of the semisubmersible floating system for phase ii of oc4* (Tech. Rep.). National Renewable Energy Lab.(NREL), Golden, CO (United States). doi: <https://doi.org/10.2172/1155123>
- Tandon, K., & Sen, S. (2025). A probabilistic integration of lstm and gaussian process regression for uncertainty-aware reservoir water level predictions. *Hydrological Sciences Journal*, 70(1), 144–161. doi: <https://doi.org/10.1080/02626667.2024.2428428>
- Thakur, A., Kumar, R., Shereena, O., Sharma, S., Li, D., & Sen, S. (2025). Integrating dl-based surrogate within an interacting particle ensemble kalman filtering framework for computationally efficient condition monitoring of fowt moorings. *Ocean Engineering*, 330, 121223. doi: <https://doi.org/10.1016/j.oceaneng.2025.121223>
- Xu, S., Guedes Soares, C., & Teixeira, Â. P. (2018). Reliability analysis of short term mooring tension of a semi-submersible system. In *International conference on offshore mechanics and arctic engineering* (Vol. 51333, p. V11BT12A029). doi: 10.1115/OMAE2018-78751
- Yang, Y., Chen, C., Liu, Q., & Liu, D. (2010, 06). *Fiber bragg grating technology used in testing tensile forces in mooring lines* (Vol. The Twentieth International Offshore and Polar Engineering Conference).